Phase Stability of Spin-Crossover Nanoparticles Investigated by Synchrotron Mössbauer Spectroscopy and Small-Angle Neutron Scattering

Mirko Mikolasek, Karl Ridier, Dimitrios Bessas, Valerio Cerantola, Gautier Félix, Grégory Chaboussant, Mario Piedrahita-Bello, José Elias Angulo-Cervera, Léa Godard, William Nicolazzi, et al.

Phase Stability of Spin-Crossover Nanoparticles investigated by Synchrotron Mössbauer Spectroscopy and Small-Angle Neutron Scattering

Mirko Mikolasek,[†] Karl Ridier,[‡] Dimitrios Bessas,[†] Valerio Cerantola,[†] Gautier Félix,[¶] Grégory Chaboussant,[§] Mario Piedrahita-Bello,[‡] Elias Angulo-Cervera,[‡] Léa Godard,[‡] William Nicolazzi,[‡] Lionel Salmon,[‡] Gábor Molnár,[‡] and Azzedine Bousseksou*[,‡]

†*ESRF-The European Synchrotron, CS40220, 38043 Grenoble Cedex 9 France*

‡*Laboratoire de Chimie de Coordination, CNRS UPR-8241 and Université de Toulouse, UPS, INP, Toulouse France*

¶*Institut Charles Gerhardt Montpellier, UMR 5253, Ingénierie Moléculaire et Nano-Objets, Université de Montpellier, ENSCM, CNRS, Place E. Bataillon, 34095 Montpellier Cedex 5, France.*

§*Laboratoire Léon Brillouin, CEA-CNRS UMR12, 91191 Gif sur Yvette, France*

E-mail: azzedine.bousseksou@lcc-toulouse.fr

Abstract

Spin-crossover nanomaterials have been actively studied in the past decade for their potential technological applications in sensing, actuating and information processing devices. Unfortunately, an increasing amount of the metallic centers becomes inactive at reduced sizes – presumably due to surface effects – limiting their switching ability and thus the scope of applications. Here we report on the investigation of 'frozen' metallic centers in nanoparticles (2 - 80 nm size) of the spin-crossover compound Fe(pyrazine)[Ni(CN)$_4$]. Magnetic measurements reveal both high-spin and low-spin residual fractions at atmospheric pressure. A pressure induced transition of the high-spin residue is observed around 1.5 GPa by synchrotron Mössbauer spectroscopy. We show that it is equivalent to a downshift of the transition temperature by ca. 400 K due to the size reduction. Unexpectedly, small-angle neutron scattering experiments demonstrate that these high-spin residual centers are not confined to the surface, which contradicts general theoretical considerations.

Graphical TOC Entry

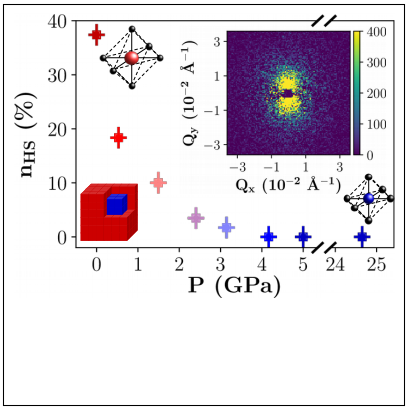

Keywords

Spin crossover nanoparticles, Phase stability, Mössbauer spectroscopy, Small-angle neutron scattering

In recent years, study of nano-objects with first-order phase transitions has raised new interesting questions since both the phase stability and the transformation kinetics are highly dependent on the object size.[1] At the nanoscale, one of the major contributions to finite-size effects is related to the large surface-to-volume ratio. Due to the surface free energies, the equilibrium conditions of surface atoms or molecules may be considerably different from those of the bulk material. This is observed in numerous well known phase transitions such as the melting process in which the melting point of nanoparticles shifts as function of the size and environment.[2] Strong surface effects can induce structural phase transition[3] or surface relaxations which may lead to topological transitions (e.g., electric, magnetic, morphological, electronic, etc.) with the size reduction.[4,5] Consequently, the characterization of the surface species is of paramount importance to understand the size-dependent properties of the material.

In the past decade, the synthesis of Spin-CrossOver (SCO)[6–8] nanomaterials and the study of size reduction and surface effects have attracted much attention.[8–18] Unfortunately, in many cases, the switching properties between the so-called low-spin (LS) and high-spin (HS) states appear strongly affected by the size reduction. In particular, an increasing fraction of the SCO centers becomes often inactive at reduced sizes, which limits the completeness of the transition and thus the scope of applications.

This effect is particularly visible in nanoparticles of Fe(II)(pyrazine)[$Ni(CN)_4$] that is a 3D-coordination network of the Hofmann clathrate family.[11,13,15] In this compound, a decrease of the cooperativity, a stabilization of the HS state and the existence of a HS residual fraction are observed at low temperature with size reduction. In addition, a LS residual fraction is also observed at high temperature for particle sizes below *ca.* 10-20 nm. Because the HS residual fraction fits with the estimated fraction of surface metallic centers, these latter were assumed to be 'frozen' in the HS state.

From a thermodynamical point of view, most observations made on SCO nanoparticules larger than *ca.* 5-10 nm can be explained by a lower surface energy of the HS state, which is

thus stabilized on the surfaces.[19] From a microscopic point of view, this stabilization of the surface metallic centers in the HS state was modelled using three different approaches. The first approach assumes *ad hoc* that surface SCO sites are frozen in the HS state,[20–23] assuming implicitly a drastic change of the ligand field of these surface metallic centers. To take more explicitly into account the underlying mechanism, other models introduced an additional surface free energy term in the Hamiltonian,[24–30] leading to potential multi-step transitions (shift of the transition temperature/pressure of the surface metallic centers) tuned by the surface energies. More recently, it was also suggested that elastic surface relaxations can be also accounted for the emergence of HS surface states. In this last approach, surface and core metallic centers are not affected by the same stress and strain, leading also to a multi-step transition.[31] Despite the predicted key role of this residual HS fraction in SCO nano-objects, to our best knowledge, there is no experimental report on the switching properties and the spatial distribution of the 'frozen' HS molecules.

In this letter, we investigate the stability and spatial distribution of the HS residual fraction in a set of nanoparticles of different sizes of the SCO compound Fe(pyrazine)[$Ni(CN)_4$] by high-pressure Synchrotron Mössbauer Spectroscopy (SMS) and POLarized Small-Angle Neutron Scattering (POLSANS).

The studied nanoparticles of Fe(pyrazine)[$Ni(CN)_4$] have a typical parallelepipedic shape with one dimension significantly shorter than the others ($a \approx b > c$). From Transmission Electronic Microscopy (TEM) and POLSANS measurements, the average in-plane and out-of-plane particle sizes were estimated to $\langle a \rangle = 41.1 \pm 6.5$ nm and $\langle c \rangle = 8 \pm 3$ nm, respectively. A second batch of particles with in-plane size $\langle a \rangle = 17.1 \pm 5.3$ nm were additionally enriched to $\sim 90\%$ in ^{57}Fe in order to carry out synchrotron Mössbauer spectroscopy with good statistics in reasonable time. Particles are embedded in a NaAOT (dioctyl sodium sulfosuccinate) polymer matrix (see ref.[15] for synthesis and characterization). The as-synthesized particles were carefully washed with ethanol and dried under vacuum. In all experiments, the particles were used in their solvated form *i.e.* without prior heat treatment.

Fe(pyrazine)[Ni(CN)$_4$] in its bulk form exhibits a first-order spin transition around 285 K.[32] As displayed in Figure 1, the LS-HS phase stability is strongly modified with size reduction, leading to a sizeable downshift of the transition temperature (ca. 263 K) and the appearance of "inactive" residual fractions since only 23% of the metallic centers exhibit SCO. It is also interesting to note that the HS residual fraction is stable down to liquid helium temperatures.

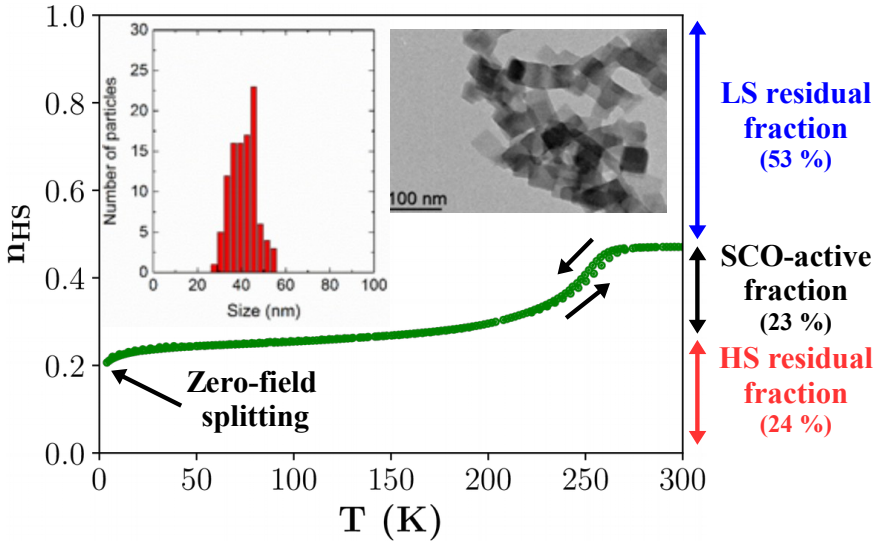

Figure 1: Thermal dependence of the HS fraction n_{HS} of the ^{56}Fe(pyrazine)[Ni(CN)$_4$] nanoparticles determined by magnetic measurements. Two Mössbauer spectra were used at 300 K ($n_{HS} = 0.47$) and 80 K ($n_{HS} = 0.24$) to calibrate the HS fraction. Below 15 K, the slight decrease of the magnetic susceptibility can be attributed to a zero-field splitting[33] (associated with magnetic anisotropy) and the HS fraction is not anymore relevant. Inset: Size-distribution histogram and selected TEM image of the particles.

Fig. 2(a) displays the Mössbauer transmission spectrum at 0.52 GPa and room temperature (298 K). The extracted isomer shifts for the HS and LS state are $IS_{HS} = 0.9 \pm 0.02$ mm/s, $IS_{LS} = 0.41 \pm 0.01$ mm/s and the quadrupole splittings $QS_{HS} = 2.01 \pm 0.03$ mm/s, $QS_{LS} = 0.57 \pm 0.01$ mm/s are in good agreement with the values reported in the literature.[15] The proportion of each spin state was extracted from the absorption areas (area under the baseline). Fig. 2(b) shows the pressure-dependence of the HS fraction at room temperature. A conversion of the HS residual fraction is observed around 1.5 GPa. Above 4 GPa, the HS fraction completely disappears. Similar observations were made with another enriched

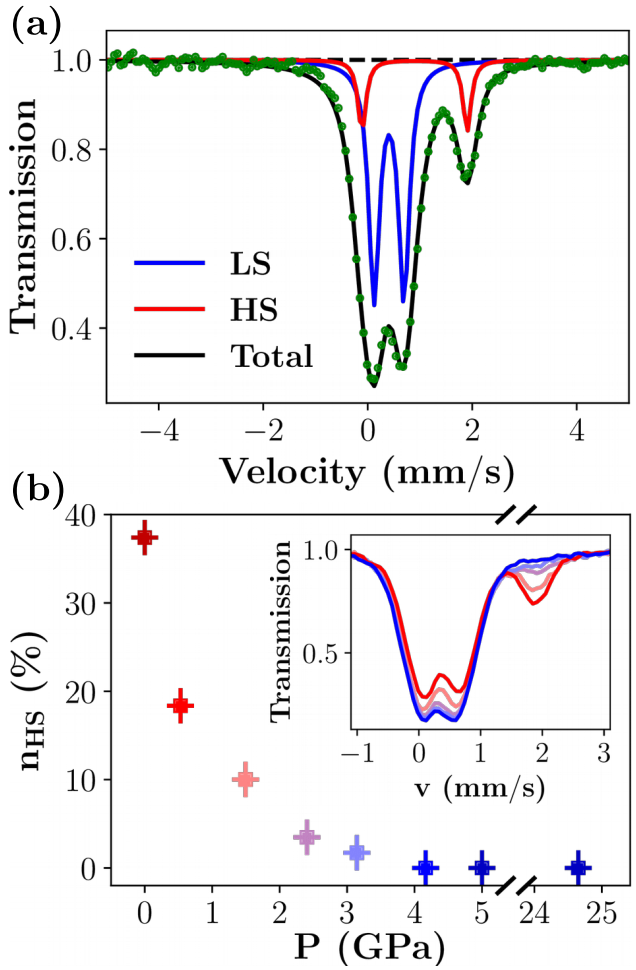

Figure 2: (a) Experimental Mössbauer spectrum obtained for ^{57}Fe(pyrazine)[Ni(CN)$_4$] particles at 0.52 ± 0.2 GPa and 298 K (green dots). The red and blue solid lines denote the contributions of the HS and LS states, respectively. The fitted curves take into account the thickness effect of the experimental spectrum. (b) Pressure dependence of the HS fraction and the corresponding Mössbauer spectra (inset).

nanoparticle sample under pressure (see Figure S6 in Supporting Information).

Taking into account the Clapeyron-slope, which links the transition temperature to the applied pressure (see the thermodynamical considerations in the SI), we can estimate that the spin transition temperature of the HS residual fraction at ambient pressure is shifted to -142 ± 118 K. (The large standard deviation is due to the experimental uncertainties of volume and entropy changes.) In other words, the HS residual centers are stabilized by *ca.* 400 K (3.3 $kJ \cdot mol^{-1}$) with respect to the bulk material due to the size reduction effect. In the present case, this strong stabilization of the HS state leads thus to an incomplete tran-

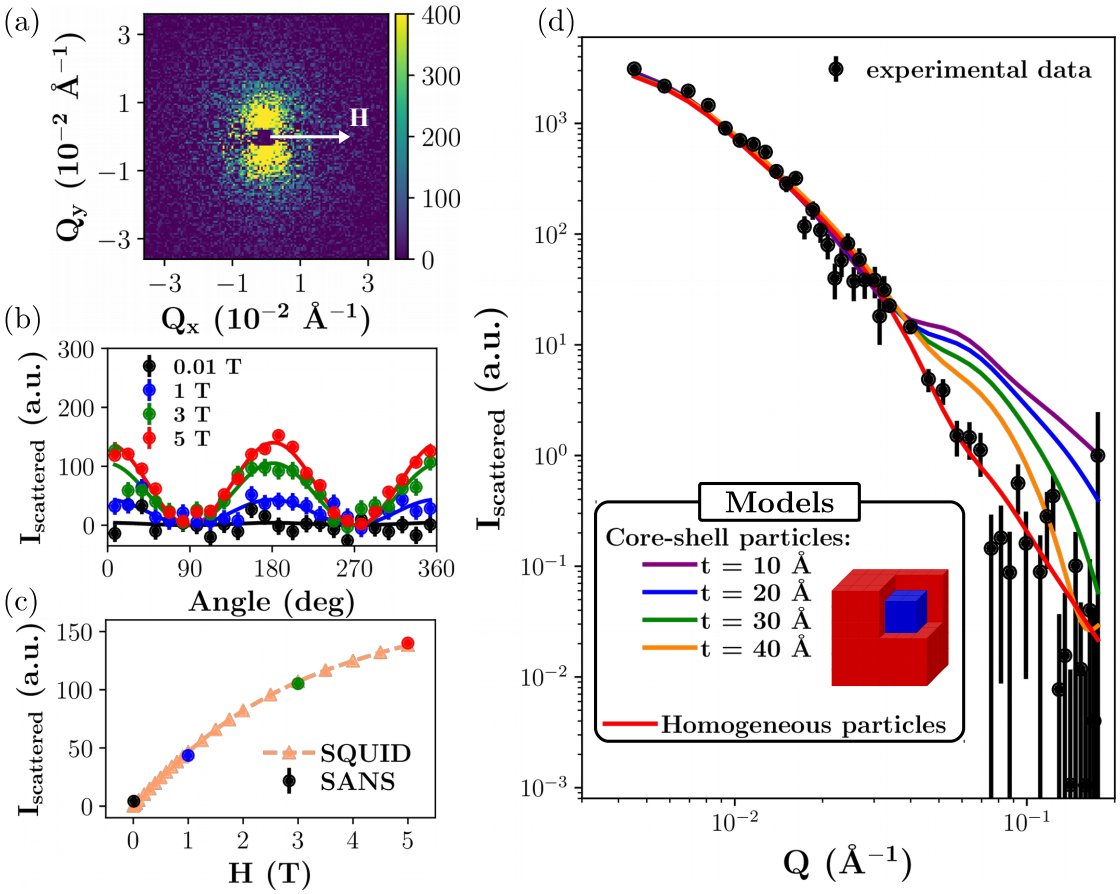

Figure 3: POLSANS measurements performed on the ^{56}Fe nanoparticles at 5 K. (a) $I_{sc}(\mathbf{Q}) = I_+(\mathbf{Q}) - I_-(\mathbf{Q})$ signal obtained on the two-dimensional detector at 5 K and under a magnetic field of 5 T. The arrow indicates the direction of the applied magnetic field. (b) Angular evolution of the scattered intensity $I_{sc}(Q)$ for various values of the magnetic field. Solid lines depict the fits using a sin^2 function as described in Equation S1. (c) Modulation amplitude of $I_{sc}(Q)$ with respect to the magnetic field. These amplitudes (circles) are compared with magnetic data obtained from SQUID measurements (triangles). (d) Magnetic form factor $F_M^2(Q)$ of the nanoparticles extracted from the measured intensities $I_+(\mathbf{Q})$ and $I_-(\mathbf{Q})$ at 5 T (see details in SI). Solid lines are the result of simulations using a core-shell parallelepiped particle model whose thickness of the magnetic shell was varied from $t = 10$ Å to that of a homogeneous magnetic parallelepiped.

sition, but our results indicate that multi-step transitions may occur in SCO nanoparticles in agreement with theoretical predictions.[24–31]

In a second step, we have characterized experimentally the spatial distribution of this paramagnetic residual HS fraction within nanoparticles of ^{56}Fe(pyrazine)[Ni(CN)$_4$] by POLSANS. This latter constitutes a technique of choice for analysing the magnetic form factor

of nano-objects in non-magnetic matrices as well as magnetic structures and correlations on the nanometer length scale.[34,35] POLSANS experiments were carried out at the PA20 spectrometer at LLB-Orphée at 5 K and under a variable magnetic field. Figure 3(a) shows the typical anisotropic signal $I_{sc}(\mathbf{Q})$ obtained on the two-dimensional detector at 5 K and 5 T, defined by the difference of the two scattered intensities $I_+(\mathbf{Q})$ and $I_-(\mathbf{Q})$ collected when neutron spins of the incoming beam are aligned antiparallel and parallel to the external magnetic field, respectively. $I_{sc}(\mathbf{Q})$ represents a magnetic-nuclear cross term which is proportional to the magnetic form factor $F_M(\mathbf{Q})$ of the nanoparticles (see details in Supporting Information).

Measurements performed under various values of the magnetic field (see Figure 3(b-c)) unambiguously demonstrate the magnetic nature of this signal, which disappears at zero field and whose magnitude follows the magnetization curve obtained from SQUID measurements at 5 K. This magnetic scattering can only originate from the SCO sites whose spin state is 'blocked' in the paramagnetic HS state at low temperature, and thus constitutes the signature, in terms of POLSANS patterns, of the residual HS fraction within the nanoparticles.

Fig. 3(d) shows the square of the magnetic form factor $F_M^2(Q)$ of the ^{56}Fe nanoparticles derived from $I_{sc}(\mathbf{Q})$ at 5 K and 5 T (see details in Supporting Information). To analyse the magnetic POLSANS data, we have considered a core-shell parallelepiped particle model in which a shell of variable thickness t only contributes to the total magnetization and where all the structural parameters (size and size distribution) are fixed to their values obtained from the analysis of the nuclear form factor of the particles $F_N^2(\mathbf{Q})$ (see Figure S4 and Table 1 in Supporting Information). When small shell thicknesses are considered, a large mismatch occurs above $Q \approx 0.04$ Å^{-1} since an enhanced scattered intensity is expected in the $Q = 2\pi/t$ range associated with the characteristic thickness t of the shell.

Fig. 3(d) shows that the simulation is substantially improved (in particular in the large-Q range) when the thickness of the magnetic shell is increased and, finally, it appears that the best fit to the data is obtained when a uniform magnetization density is considered

throughout the particles. Similar results were obtained for two other non-enriched particle batches with different sizes $\langle a \rangle = 14.4 \pm 1.7$ nm and 79.1 ± 16.9 nm (see Figure S5 in Supporting Information).

These POLSANS results tend to show that the magnetization associated with the residual HS sites is uniformly distributed within the particles rather than concentrated at the surface. These experimental observations are in disagreement with the theoretical predictions, but obviously call for further confirmations through different experimental techniques.

In the case of the present 3D-coordination network particles, an important aspect is the presence of both HS and LS residual fractions. While the general thermodynamical trend would be the stabilization of the HS state on the surface due to its lower surface energy, we may suggest that the coordination of certain species as well as the existence of surface distortions/deformations might be possible contributions that favor the strong ligand field configuration (LS state) on the particle surface. As for the residual HS fraction and by analogy with Prussian blue analogue materials in which the influence of lattice defects and vacancies is well established,[36,37] the porous 3D network may contain defects and/or guest molecules, which may locally stabilize the HS state of a certain amount of iron ions within the whole particle volume.

In conclusion, we have studied the stability and the spatial distribution of the high-spin residual fraction in spin-crossover nanoparticles of Fe(pyrazine)[$Ni(CN)_4$] by synchrotron high-pressure Mössbauer spectroscopy and polarized small-angle neutron scattering. These experiments revealed that the 'frozen' HS centers are actually SCO active and can be switched to the LS state at room temperature by applying a pressure of 1.5 GPa. This result indicates that initially fully LS materials can become SCO active at reduced sizes. Surprisingly, the HS residual centers appear homogeneously distributed within the particles - in contrast to what is assumed in general from theoretical considerations. We have tentatively ascribed this finding to the particular porous 3D network structure of the investigated compound. While these considerations remain necessarily speculative at this stage, our results clearly show

that beyond the general considerations of phase stability, the specific chemistry and crystal structure of each SCO compound must be carefully taken into account when interpreting size effects. Powerful experimental techniques, such as POLSANS, will certainly play an increasing role in this respect in the future.

Acknowledgement

The European Synchrotron Radiation Facility (ESRF) is acknowledge for beamtime provision at the Nuclear Resonance beamline ID18. The authors thank Jeroen Jacobs and Jean-Philippe Celse for their technical assistance during the high-pressure experiment as well as Aleksandr I. Chumakov and Rudolf Rüffer for helpful discussions. The authors also thank Nicolas Martin for his technical help with SANS experiments. This work was partially founded by the European Commission through the SPINSWITCH project (H2020-MSCA-RISE-2016, Grant Agreement No. 734322). MPB and EAC thank the Federal University of Toulouse and the CONACYT, respectively, for their PhD grants.

Supporting Information Available

The following files are available free of charge.

- SI.tex: this file contains the results for the other studied samples, additional information about POLSANS and the full description of the thermodynamical model.

References

(1) Sun, C. Q. Size dependence of nanostructures: Impact of bond order deficiency. *Prog. Solid. State. Ch.* **2007**, *35*, 1–159.

(2) Lu, K.; Jin, Z. Melting and superheating of low-dimensional materials. *Curr. Opin. Solid. St. M.* **2001**, *5*, 39–44.

(3) Ranade, M. R.; Navrotsky, A.; Zhang, H. Z.; Banfield, J. F.; Elder, S. H.; Zaban, A.; Borse, P. H.; Kulkarni, S. K.; Doran, G. S.; Whitfield, H. J. Energetics of nanocrystalline TiO2. *PNAS* **2002**, *99*, 6476–6481.

(4) Kodama, R. H.; Berkowitz, A. E.; McNiff, E. J.; Foner, S. Surface spin disorder in ferrite nanoparticles (invited). *J. Appl. Phys.* **1997**, *81*, 5552–5557.

(5) Noguera, C.; Goniakowski, J. Polarity in Oxide Nano-objects. *Chem. Rev.* **2013**, *113*, 4073–4105.

(6) Gütlich, P.; Hauser, A.; Spiering, H. Thermal and Optical Switching of Iron(II) Complexes. *Angew. Chem. Int. Ed. Engl.* **1994**, *33*, 2024–2054.

(7) Halcrow, M. A., Ed. *Spin-Crossover Materials: Properties and Applications*; John Wiley & Sons Ltd: Oxford, UK, 2013.

(8) Mikolasek, M.; Manrique-Juarez, M. D.; Shepherd, H. J.; Ridier, K.; Rat, S.; Shalabaeva, V.; Bas, A.-C.; Collings, I. E.; Mathieu, F.; Cacheux, J. et al. Complete Set of Elastic Moduli of a Spin-Crossover Solid: Spin-State Dependence and Mechanical Actuation. *J. Am. Chem. Soc.* **2018**, *140*, 8970–8979.

(9) Molnár, G.; Rat, S.; Salmon, L.; Nicolazzi, W.; Bousseksou, A. Spin Crossover Nanomaterials: From Fundamental Concepts to Devices. *Adv. Mater.* **2018**, *30*, 1703862.

(10) Mikolasek, M.; Félix, G.; Nicolazzi, W.; Molnár, G.; Salmon, L.; Bousseksou, A. Finite size effects in molecular spin crossover materials. *New J. Chem.* **2014**, *38*, 1834–1839.

(11) Volatron, F.; Catala, L.; Rivière, E.; Gloter, A.; Stéphan, O.; Mallah, T. Spin-Crossover Coordination Nanoparticles. *Inorg. Chem.* **2008**, *47*, 6584–6586.

(12) Bairagi, K.; Bellec, A.; Fourmental, C.; Iasco, O.; Lagoute, J.; Chacon, C.; Girard, Y.; Rousset, S.; Choueikani, F.; Otero, E. et al. Temperature-, Light-, and Soft X-ray-Induced Spin Crossover in a Single Layer of FeII-Pyrazolylborate Molecules in Direct Contact with Gold. *J. Phys. Chem. C* **2018**, *122*, 727–731.

(13) Larionova, J.; Salmon, L.; Guari, Y.; Tokarev, A.; Molvinger, K.; Molnár, G.; Bousseksou, A. Towards the Ultimate Size Limit of the Memory Effect in Spin-Crossover Solids. *Angew. Chem. Int. Ed.* **2008**, *47*, 8236–8240.

(14) Luo, Y.-H.; Chen, C.; Lu, G.-W.; Hong, D.-L.; He, X.-T.; Wang, C.; Wang, J.-Y.; Sun, B.-W. Atomically Thin Two-Dimensional Nanosheets with Tunable Spin-Crossover Properties. *J. Phys. Chem. Lett.* **2018**, *9*, 7052–7058.

(15) Peng, H.; Tricard, S.; Félix, G.; Molnár, G.; Nicolazzi, W.; Salmon, L.; Bousseksou, A. Re-Appearance of Cooperativity in Ultra-Small Spin-Crossover [Fe(pz){Ni(CN)4}] Nanoparticles. *Angew. Chem. Int. Ed.* **2014**, *53*, 10894–10898.

(16) Groizard, T.; Papior, N.; Le Guennic, B.; Robert, V.; Kepenekian, M. Enhanced Cooperativity in Supported Spin-Crossover Metal–Organic Frameworks. *J. Phys. Chem. Lett.* **2017**, *8*, 3415–3420.

(17) Shalabaeva, V.; Mikolasek, M.; Manrique-Juarez, M. D.; Bas, A.-C.; Rat, S.; Salmon, L.; Nicolazzi, W.; Molnár, G.; Bousseksou, A. Unprecedented Size Effect on the Phase Stability of Molecular Thin Films Displaying a Spin Transition. *J. Phys. Chem. C* **2017**, *121*, 25617–25621.

(18) Ossinger, S.; Naggert, H.; Kipgen, L.; Jasper-Toennies, T.; Rai, A.; Rudnik, J.; Nickel, F.; Arruda, L. M.; Bernien, M.; Kuch, W. et al. Vacuum-Evaporable Spin-Crossover Complexes in Direct Contact with a Solid Surface: Bismuth versus Gold. *J. Phys. Chem. C* **2017**, *121*, 1210–1219.

(19) Félix, G.; Nicolazzi, W.; Salmon, L.; Molnár, G.; Perrier, M.; Maurin, G.; Larionova, J.; Long, J.; Guari, Y.; Bousseksou, A. Enhanced Cooperative Interactions at the Nanoscale in Spin-Crossover Materials with a First-Order Phase Transition. *Phys. Rev. Lett.* **2013**, *110*, 235701.

(20) Muraoka, A.; Boukheddaden, K.; Linarès, J.; Varret, F. Two-dimensional Ising-like model with specific edge effects for spin-crossover nanoparticles: A Monte Carlo study. *Phys. Rev. B* **2011**, *84*, 054119.

(21) Atitoaie, A.; Tanasa, R.; Enachescu, C. Size dependent thermal hysteresis in spin crossover nanoparticles reflected within a Monte Carlo based Ising-like model. *J. Magn. Magn. Mater.* **2012**, *324*, 1596–1600.

(22) Oubouchou, H.; Slimani, A.; Boukheddaden, K. Interplay between elastic interactions in a core-shell model for spin-crossover nanoparticles. *Phys. Rev. B* **2013**, *87*, 104104.

(23) Slimani, A.; Boukheddaden, K.; Yamashita, K. Thermal spin transition of circularly shaped nanoparticles in a core-shell structure investigated with an electroelastic model. *Phys. Rev. B* **2014**, *89*, 214109.

(24) Chiruta, D.; Linares, J.; Dimian, M.; Alayli, Y.; Garcia, Y. Role of Edge Atoms in the Hysteretic Behaviour of 3D Spin Crossover Nanoparticles Revealed by an Ising-Like Model: Role of Edge Atoms in the Hysteretic Behaviour of 3D SCO Nanoparticles. *Eur. J. Inorg. Chem.* **2013**, *2013*, 5086–5093.

(25) Félix, G.; Nicolazzi, W.; Mikolasek, M.; Molnár, G.; Bousseksou, A. Non-extensivity of thermodynamics at the nanoscale in molecular spin crossover materials: a balance between surface and volume. *Phys. Chem. Chem. Phys.* **2014**, *16*, 7358–7367.

(26) Chiruta, D.; Linares, J.; Richard Dahoo, P.; Dimian, M. Influence of pressure and interactions strength on hysteretic behavior in two-dimensional polymeric spin crossover compounds. *Physica B* **2014**, *435*, 76–79.

(27) Chiruta, D.; Linares, J.; Garcia, Y.; Dimian, M.; Dahoo, P. R. Analysis of multi-step transitions in spin crossover nanochains. *Physica B* **2014**, *434*, 134–138.

(28) Chiruta, D.; Jureschi, C.-M.; Linares, J.; Dahoo, P. R.; Garcia, Y.; Rotaru, A. On the origin of multi-step spin transition behaviour in 1D nanoparticles. *Eur. Phys. J. B* **2015**, *88*, 233.

(29) Guerroudj, S.; Caballero, R.; De Zela, F.; Jureschi, C.; Linares, J.; Boukheddaden, K. Monte Carlo - Metropolis Investigations of Shape and Matrix Effects in 2D and 3D Spin-Crossover Nanoparticles. *J. Phys. Conf. Ser.* **2016**, *738*, 012068.

(30) Mikolasek, M.; Nicolazzi, W.; Terki, F.; Molnár, G.; Bousseksou, A. Investigation of surface energies in spin crossover nanomaterials: the role of surface relaxations. *Phys. Chem. Chem. Phys.* **2017**, *19*, 12276–12281.

(31) Mikolasek, M.; Nicolazzi, W.; Terki, F.; Molnár, G.; Bousseksou, A. Surface transition in spin crossover nanoparticles. *Chem. Phys. Lett.* **2017**, *678*, 107–111.

(32) Niel, V.; Martinez-Agudo, J. M.; Muñoz, M. C.; Gaspar, A. B.; Real, J. A. Cooperative Spin Crossover Behavior in Cyanide-Bridged Fe(II)-M(II) Bimetallic 3D Hofmann-like Networks (M = Ni, Pd, and Pt). *Inorg. Chem.* **2001**, *40*, 3838–3839.

(33) Kahn, O. *Molecular magnetism*; VCH: New York, NY, 1993; OCLC: 246619402.

(34) Disch, S.; Wetterskog, E.; Hermann, R. P.; Wiedenmann, A.; Vainio, U.; Salazar-Alvarez, G.; Bergström, L.; Brückel, T. Quantitative spatial magnetization distribution in iron oxide nanocubes and nanospheres by polarized small-angle neutron scattering. *New J. Phys.* **2012**, *14*, 013025.

(35) Krycka, K. L.; Booth, R. A.; Hogg, C. R.; Ijiri, Y.; Borchers, J. A.; Chen, W. C.; Watson, S. M.; Laver, M.; Gentile, T. R.; Dedon, L. R. et al. Core-Shell Magnetic

Morphology of Structurally Uniform Magnetite Nanoparticles. *Phys. Rev. Lett.* **2010**, *104*, 207203.

(36) Vertelman, E. J. M.; Maccallini, E.; Gournis, D.; Rudolf, P.; Bakas, T.; Luzon, J.; Broer, R.; Pugzlys, A.; Lummen, T. T. A.; van Loosdrecht, P. H. M. et al. The Influence of Defects on the Electron-Transfer and Magnetic Properties of RbxMn[Fe(CN)6]y·zH2O. *Chem. Mater.* **2006**, *18*, 1951–1963.

(37) Bleuzen, A.; Escax, V.; Ferrier, A.; Villain, F.; Verdaguer, M.; Münsch, P.; Itié, J.-P. Thermally induced electron transfer in a CsCoFe Prussian blue derivative: the specific role of the alkali-metal ion. *Angew. Chem. Int. Ed.* **2004**, *43*, 3728–3731.